Compensation of Linear Distortions by Using XPM With Parabolic Pulses as a Time Lens

Trina T. Ng, Francesca Parmigiani, Morten Ibsen, Zhaowei Zhang, Periklis Petropoulos, and David J. Richardson

***Abstract*—We experimentally demonstrate an all-optical all-fiberized scheme that can eliminate linear perturbations in the time domain. The technique relies on performing optical Fourier transforms on distorted signals to move their distortions from the time to the frequency domain. A near-complete transformation is obtained by using cross-phase modulation with parabolic pulses as a time lens. Mitigation of second- and third-order dispersed pulses is demonstrated as well as good transform behaviour.**

***Index Terms*—Optical phase modulation, optical Fourier transformation (OFT), waveform distortion elimination, parabolic pulses.**

I. Introduction

SHORT optical pulses, when transmitted over large distances, are susceptible to a range of linear optical distortions including chromatic dispersion, polarization-mode dispersion, and timing jitter. With data rates increasing to 40 Gb/s and above, such distortions have an increasing impact on signal quality. Furthermore, temperature changes and reconfigurable networks can lead to fluctuations in the amount of residual distortion accumulated through a transmission link.

Temporal optical Fourier transforms (TOFTs) could potentially be used to mitigate multiple linear distortions in signals all-optically, and without prior knowledge of the amount of distortion suffered. A complete TOFT causes the temporal and spectral envelopes of the target signal to swap, with a magnification factor. Thus, signals which exhibit similar shapes in both domains, such as Gaussian or sech^2 pulses, can be completely reconstructed after experiencing linear distortions, by taking on the form of its unchanged spectral envelope. Conversely, the temporal distortion is then projected into the spectral domain. Previously, this compensation technique was analytically and experimentally investigated by using an electrooptic phase modulator to create a time lens in analogy to spatial Fourier transforms [1], [2]. However, a time lens analogy would be better approximated by a quadratic phase shift rather than the sinusoidal phase shift applied by phase modulators [2], [3]. We have previously demonstrated temporal optical Fourier transforms of pulses distorted by second- and third-order dispersed pulses, using cross-phase modulation (XPM) with parabolic pulses to generate a quadratic phase shift [3]. Parabolic pulses were generated in a passive and stable manner using a super-structured fiber Bragg grating (SSFBG).

Manuscript received December 20, 2007; revised March 19, 2008.

The authors are with the Optoelectronics Research Centre, University of Southampton, SO17 1BJ Southampton, U.K. (e-mail: ttn@orc.soton.ac.uk).

Color versions of one or more of the figures in this letter are available online at http://ieeexplore.ieee.org.

Digital Object Identifier 10.1109/LPT.2008.924304

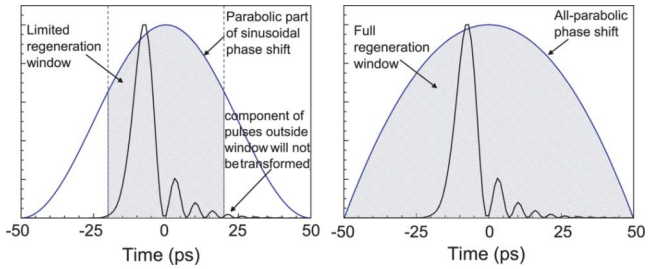

Fig. 1. Parabolic phase modulation can provide a wider regenerating window and more complete regeneration than using a sinusoidal phase modulation.

In this letter, we investigate this phenomenon further through a more thorough theory and numerical simulation. Furthermore, we present here a more complete set of results to clearly demonstrate the TOFT behaviour of our device. As before, the technique is demonstrated at 10 Gb/s; however, since it is all-optical and relies on fiber nonlinearities to apply the quadratic phase shift, it should readily be scalable to much higher repetition rates.

II. Operational Principle

The linear distortion compensator operates by performing a TOFT on the distorted pulse. The TOFT replaces the pulses' distorted temporal waveform with its spectral envelope, which for most linear perturbations remains greatly undistorted.

TOFT can be achieved in an analogous way to diffraction patterns [4], in which a spatial quadratic phase shift is applied by a lens to create a linear spatial chirp. The waveform then diffracts in space to take the Fourier transformed profile of its aperture shape at the focal length where the induced linear chirp is fully compensated. This can be emulated in the temporal domain by applying a temporal quadratic phase shift (time lens) to the target pulse and observing the pulse after a matched amount of dispersion given by [5]

$$K = -\frac{d^2\phi}{dt^2} = \frac{1}{\beta_2 L} \tag{1}$$

where K is the chirp rate applied to the target pulse, ϕ is the applied phase shift, and $\beta_2 L$ is the following dispersion. Thus, a sinusoidal phase shift which is close to parabolic over only a limited range of the clock period, will induce a chirp that cannot be completely compensated for by a length of dispersive fiber. Any parts of the pulse extending beyond the parabolic region will not be properly transformed and only the section of the target pulse sitting within the parabolic region will be compensated. Fig. 1 shows the increased compensating window that can be obtained with a parabolic phase shift as compared to a sinusoidal one.

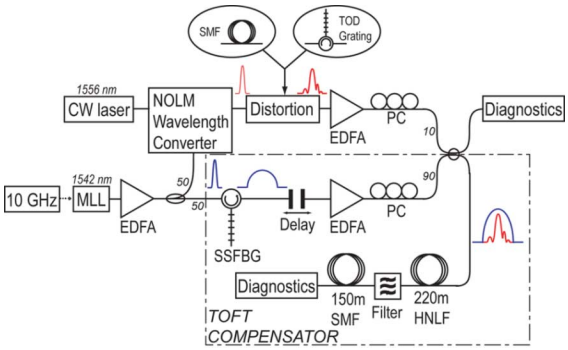

Fig. 2. Experimental setup of the Fourier transform compensator. PC: Polarization controller.

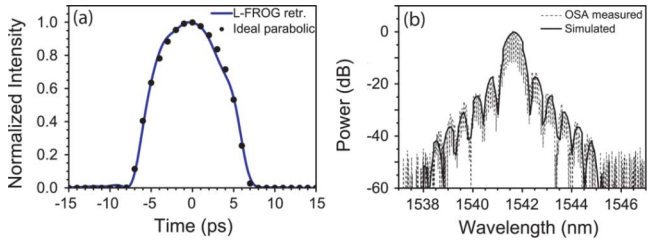

Fig. 3. (a) Temporal profile of the parabolic pulse as compared to an ideal 10-ps parabola. (b) Spectral response of the SSFBG.

As in optical imaging, the scale of the Fourier transformed waveform is determined by the gradient of the phase shift induced by the lens and is given by $t = \omega\beta_2 L$. That is, using a higher K and lower $\beta_2 L$ in (1) will result in a (temporally) narrower pulse. Recovery of the original pulsewidth can then be achieved if the condition $K = 1/\Delta t_0^2$ is satisfied, where Δt_0 is the transform-limited width of the input pulse. Furthermore, to perform a complete transformation, the phase shift must induce a chirp rate $K \gg \Delta\omega^2$, where $\Delta\omega$ is the spectral bandwidth of the signal [1]. The compensation available when using commercial phase modulators is, therefore, restricted by the chirp rate it can induce with its V_π and the amount of voltage that can be applied to it.

We overcome these limitations here by using XPM between the target pulses and parabolic pulses to induce the required quadratic phase shift. The XPM induces a chirp on the target pulse which is proportional to the gradient of the parabolic pulse intensity profile. This allows us to easily adjust K by increasing the power of the parabolic pulses.

III. Experiment

The experimental setup and operation principle of the scheme is shown in Fig. 2. Pulses from a 2-ps 10-GHz mode-locked erbium fiber ring laser (MLL) operating at 1542 nm were first split into two paths using a 50 : 50 coupler. One path was wavelength-converted in a nonlinear optical loop mirror (NOLM), thus generating 3-ps pulses at a wavelength of 1556 nm [6]. These pulses were subsequently distorted using either second-order dispersion [group-velocity dispersion (GVD)] in a length of single-mode fiber (SMF), or third-order distortion imposed by a fiber Bragg grating (FBG), to form the target signal to be processed.

In the second path we generate parabolic pump pulses for the time lens. These parabolic pulses were generated using pulse shaping in an SSFBG. The shaped pulses were designed to have a 10-ps [full-width at half-maximum (FWHM)] parabolic envelope superimposed upon a fifth-order super-Gaussian profile to reduce their spectral extent. The parabolic pulses generated in this way have previously been successfully used for phase modulation in a retiming scheme [7]. Fig. 3(a) shows the temporal profile of the measured pulses as compared to an ideal parabolic pulse. The good agreement between the measured and the ideal pulses confirm that that the intensity profile of our shaped pulses had an almost linear gradient which in turn should induce a linear chirp on our distorted pulses. The reflected pulse spectrum is given in Fig. 3(b) showing the spectral shaping imposed by the SSFBG. Characterization of the pulses reflected off the SSFBG were obtained using a linear frequency-resolved gating (L-FROG) technique [8]. After generation the parabolic pulses were amplified using an erbium-doped fiber amplifier (EDFA) and coupled together with the distorted pulses using a 90 : 10 coupler.

An optical delay line in the path of the parabolic pump was used to ensure the signal and pump pulses were overlapping temporally before being launched into 220 m of highly nonlinear fiber (HNLF). The HNLF has a nonlinear coefficient of 20 $\mathrm{W}^{-1} \cdot \mathrm{km}^{-1}$ and a zero-dispersion wavelength at 1550 nm, which ensured minimum walk-off between the two signals. While the power of the parabolic pump pulses could be varied, the power of the distorted pulses was kept low to avoid spectral broadening from self-phase modulation. During propagation in the HNLF, the distorted signal acquired a linear chirp due to XPM induced by the much stronger parabolic pulses. After the HNLF, the parabolic pulses are filtered out by a 3-nm bandpass filter centered at 1556 nm, and the target signal launched into 150 m of SMF to compensate for the induced linear chirp and complete the transformation [1].

IV. Results

We tested the operation of our compensation system using clean and GVD-distorted target pulses. According to (1), our parabolic pump pulses required an average power of 19.5 dBm to generate a chirp rate, $K = -3.4 \times 10^{23}\ \mathrm{s}^{-2}$, to inversely match the dispersion, $\beta_2 L = -3 \times 10^{-24}\ \mathrm{s}^2$, arising from 150 m of SMF. Preservation of the spectrum in dispersed pulses implies that after TOFT they should all emerge temporally identical to each other regardless of their input distortion. This behaviour would not be observed for other types of compression in which different input distortions will experience different transformed widths. Thus, we can confirm the matching condition by observing the change in pulsewidth of the target pulses at the output of the compensator as the pump power is increased. This is shown in Fig. 4 (lines) where we have simulated the plot of output pulsewidth against average pump power for target pulses with different levels of distortion. We see that all the output pulses converge to the same width near the calculated pump power indicating the operational point for TOFT. Our measurements of the system as shown by Fig. 4 (symbols) confirm this and agree reasonably well with our simulations, intersecting near the predicted power level.

The GVD-distorted pulses at the input and output of the compensator operating at the TOFT point are shown in Fig. 5. Fig. 5(a) shows the autocorrelations of the input pulses with no

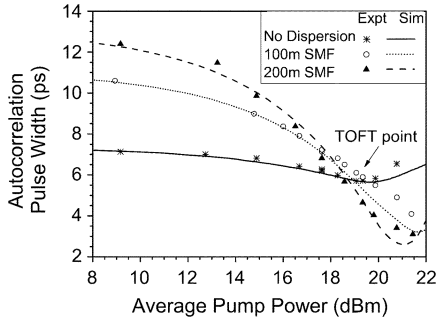

Fig. 4. Dependence of the output pulsewidth on the pump power for various values of GVD distortion, indicating the correct operating point for TOFT.

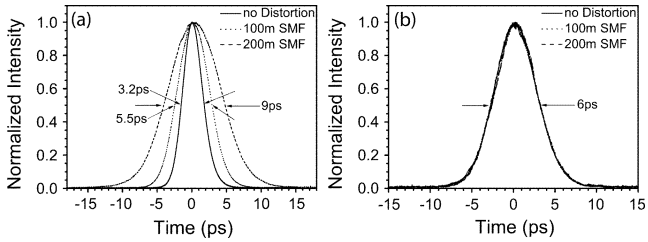

Fig. 5. Autocorrelation traces of the three cases of GVD-distorted pulses (a) at the input of the compensating system and (b) at the output of the compensating system. Nb: the labelled widths refer to the FWHM of the autocorrelation traces rather than the FWHM of the pulse intensity profiles.

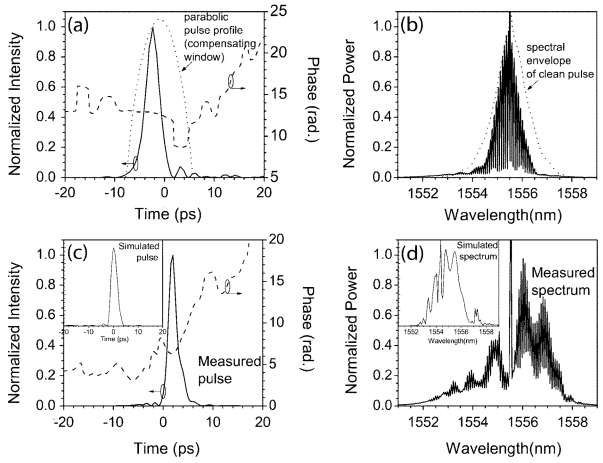

Fig. 6. (a) Temporal profile and (b) spectrum of the TOD-distorted pulses at the input of the TOFT compensator. At the output of the TOFT compensator, the (c) temporal profile and (d) spectrum of the TOD-distorted pulses have swapped. Shape of output spectrum is imperfect due to leakage outside the parabolic window, but has expected shape compared to simulation.

dispersion and those dispersed by 100 and 200 m of SMF. After compensation, all the pulses have the same autocorrelation width of 6 ps regardless of the GVD at the input, as shown in Fig. 5(b). This output width could potentially be reduced by using a different (but still matched) chirp and dispersion pair, that is, by increasing the pump power and shortening the SMF at the output.

We then proceeded to apply TOFT to pulses distorted by third-order dispersion (TOD) using the same setup. Our pulses were distorted by reflection from a pair of FBGs, designed to affect only the time delay of the frequency components of the signal. Fig. 6(a) shows the L-FROG characterization of the pulses reflected off the FBGs. The dotted line shows a 10-ps apodized parabolic pulse profile which can be seen to cover most of the distorted pulse but not all. Thus, we would not expect parts of the TOD pulse extending outside the parabolic envelope to be transformed. In Fig. 6(b) we see that the pulse spectrum has experienced some minor filtering from the TOD gratings as compared to the original pulse. The spectrum is otherwise largely unchanged. Fig. 6(c) and (d) shows the corresponding temporal and spectral traces at the output of the device. In Fig. 6(c), the temporal pulse can be seen to be compressed and exhibits a waveform resembling the profile of the input spectrum in (b). Fig. 6(d) shows the transformed output spectrum to which the main temporal distortions have been passed. Although the spectrum does show ringing features resembling the distorted input pulse, it is clear that the transformation in the spectral domain is imperfect. This is, due to the limited TOFT window provided by our 10-ps parabolic pulses. Any parts of the distorted pulse outside of this window did not experience the linear chirp which resulted in imperfect transformation. The simulated converted pulse and spectrum using the apodized parabolic in Fig. 6(a) is shown in the inset for comparison.

V. Conclusion

We have experimentally demonstrated the mitigation of second- and third-order dispersion of short optical pulses by using a combination of XPM induced in HNLF by SSFBG-shaped parabolic pulses and matching dispersion. The intensity profile of the parabolic pulses ensures that the chirp is linear over the full modulation window, so that it can be properly compensated for by a dispersive medium. By appropriately modifying the SSFBG design, or by adopting nonlinear techniques for the generation and broadening of the parabolic pulses [8], it should be possible to extend the temporal window of operation, thus enabling mitigation of more severe pulse distortions.

References

[1] T. Hirooka and M. Nakazawa, "Optical adaptive equalization of high-speed signals using time-domain optical Fourier transformation," *J. Lightw. Technol.*, vol. 24, no. 7, pp. 2530–2540, Jul. 2006.

[2] M. Nakazawa and T. Hirooka, "Distortion-free pulse transformation using the time-domain optical Fourier transformation and transform limited optical pulses," *J. Opt. Soc. Amer. B*, vol. 22, no. 9, pp. 1842–1855, 2005.

[3] T. T. Ng, F. Parmigiani, M. Ibsen, Z. Zhang, P. Petropoulos, and D. J. Richardson, "Linear-distortion compensation using XPM with parabolic pulses," in *Optical Fibre Communications Conf.*, Mar. 2007, vol. JWA58.

[4] H. Hakimi, F. Hakimi, K. L. Hall, and K. A. Rauschenbach, "A new wideband pulse-restoration technique for digital fiber-optic communication systems using temporal gratings," *IEEE Photon. Technol. Lett.*, vol. 11, no. 8, pp. 1048–1050, Aug. 1999.

[5] B. H. Kolner, "Space-time duality and the theory of temporal imaging," *IEEE J. Quantum Electron.*, vol. 30, no. 8, pp. 1951–1963, Aug. 1994.

[6] F. Parmigiani, P. Petropoulos, M. Ibsen, and D. J. Richardson, "All-optical pulse reshaping and retiming systems incorporating pulse shaping fibre Bragg gratings," *J. Lightw. Technol.*, vol. 24, no. 1, pp. 357–364, Jan. 2006.

[7] F. Parmigiani, P. Petropoulos, M. Ibsen, and D. J. Richardson, "Pulse retiming based on XPM using parabolic pulses formed in a fiber Bragg grating," *IEEE Photon. Technol. Lett.*, vol. 18, no. 7, pp. 829–831, Apr. 1, 2006.

[8] C. Finot, L. Provost, P. Petropoulos, and D. J. Richardson, "Parabolic pulse generation through passive nonlinear pulse reshaping in a normally dispersive two segment fiber device," *Opt. Express*, vol. 15, no. 3, pp. 852–864, 2007.